

A Diagnostic Study of Formation and Structures of the Meiyu Front System over East Asia

Yushu ZHOU, Shouting GAO and Samuel S.P. SHEN

Laboratory of Cloud-Precipitation Physics and Severe Storms, Institute of Atmospheric Physics, Chinese Academy of Sciences, Beijing, China

(Manuscript received 14 May 2001, in final form 27 August 2004)

Abstract

The concept of a dew-point front was introduced, and its existence was identified near the periphery of the west Pacific subtropical anticyclone by using the daily $1^\circ \times 1^\circ$ data of the National Center for Environmental Prediction/National Center for Atmospheric Research (NCEP/NCAR). The dew-point front was a transitional belt between the moist southwest monsoon flow and the dry adiabatic sinking flow, marked by a large horizontal moisture gradient in the mid-lower troposphere. The dew-point front and the Meiyu front, to its north side, formed the Meiyu front system (MYFS). The Meiyu front was the north branch of the MYFS, and extended northward in the mid-lower troposphere. The dew-point front was the south branch of the MYFS, located between 500 hPa and 700 hPa. Along the dew-point front (Meiyu), westerly (easterly) and easterly (westerly) winds prevailed in the lower (upper) and upper (lower) troposphere respectively. Strong ascending motion in the passageway between the two fronts was surrounded by subsidence. Further, a frontogenesis function was used to diagnose the frontogenesis of the MYFS. The analysis indicated that the convergence and deformation of the horizontal wind were important factors responsible for both the formation and development of the Meiyu front and the dew-point front.

1. Introduction

During June and July, from the Mid-lower Reaches of the Yangtze River (MRYS) in China to Southwestern Japan, a precipitation zone occurs and lasts for two to three weeks with a high probability for torrential rains. This phenomenon is called the ‘Meiyu’ in China and the ‘Baiu’ in Japan. In the period of Meiyu, the precipitation is excessively intensive, and serious floods often occur over the MRYS. The floods cause tremendous damage to infrastructure, industry, agriculture, and human lives.

Recent Chinese history has recorded massive floods occurring in 1954, 1991, 1998, and 1999 over the MRYS. Therefore, the Meiyu has always been one of important meteorological research topics. For geographic reasons, meteorologists in China and Japan have particular interests in the Meiyu (Tao 1958; Lin 1979; Ninomiya and Yamazaki 1979; Zhang and Zhang 1990). Previous research shows that the Meiyu is caused mainly by the Meiyu front (or “Baiu front” in Japan)—a quasi-stationary front oriented in the northeast-southwest direction at the lower troposphere. Chinese and Japanese meteorologists have studied various aspects of the Meiyu front (Akiyama 1973, 1984, 1987, 1989, 1990; Gao et al. 1990; Hu 1997; Matsumoto et al. 1970, 1971; Iwasaki and Takeda 1993; Ninomiya 1984, 1999; Ninomiya and Kurihara 1987; Ninomiya and Akiyama 1992; Ninomiya et al. 1988), and concluded that (i)

Corresponding author address: Gao Shouting, Laboratory of Cloud-Precipitation Physics and Severe Storms, Institute of Atmospheric Physics, Chinese Academy of Sciences, Beijing 100029, China.
E-mail: gst@lasg.iap.ac.cn
© 2004, Meteorological Society of Japan

the Meiyu front is a belt with a large humidity gradient stretching along the MRYS from China to Japan; (ii) the Meiyu front should be expressed by a very dense gradient zone of equivalent potential temperature (θ_e) isolines rather than by a dense gradient zone of temperature (T) isolines; (iii) the Meiyu front should be classified as a subtropical front with a multi-scale (large, synoptic and mesoscale) structure; (iv) convective activities often occur along the Meiyu front; and (v) the Meiyu front is related to the subtropical anticyclone, the South Asia anticyclone, the blocking anticyclone at mid-high latitudes, the southwest monsoon flow, the low-level jet (LLJ), the upper-level jet, and other large-scale atmospheric phenomena. Matsumoto et al. (1971) pointed out that the Meiyu front is a warm-moist band lying at the mid-troposphere, accompanied by a strong cyclonic shear and neutral thermodynamic stratification. Akiyama's studies (1989, 1990) revealed that the features of the Meiyu front in China are not always the same as those in Japan or in the Northwest Pacific. First, the Meiyu front over continental China is a meeting zone between the summer monsoon air mass ($\theta_e \geq 340$ K) and the mid-latitude air mass ($320 \text{ K} \leq \theta_e \leq 330$ K). This front has a strong horizontal wind shear and a weak baroclinicity. Second, the Meiyu front over the northwest Pacific is a meeting zone between the tropical air mass ($330 \text{ K} < \theta_e < 340$ K) and the polar air mass ($\theta_e < 320$ K) and has a relatively strong baroclinicity and a strong vertical wind shear. Third, the Meiyu front over Japan is a transitional zone between the Northwest Pacific Meiyu front and the continental China Meiyu front. Ninomiya et al. (1992) studied the multi-scale features of the Meiyu front, and presented a schematic diagram of the large-scale circulation around it. Kitabatake (2000) studied the structure of the Meiyu front over continental China and emphasized that the dryline-like front at lower levels could couple with an upper front through the combination of cold and warm flows at middle levels. This coupling is favorable to the occurrence of severe convective clouds.

As the Meiyu front is closely related to Meiyu precipitation, meteorologists need to understand the Meiyu front's formation, structure, and clouds in order to predict the Meiyu's

precipitation reliably. Such a forecast, however, has not been satisfactory, even with the help of satellite data. Current operational forecasts focus mainly on the Meiyu front, which reflects only a convergence zone caused by the confluence of the summer monsoon in East Asia and the dry-warm air over the rest of Asia, and this zone is only one aspect of the adjustment of the atmospheric circulation in East Asia. Another important aspect is the northward movement and westward extension of the west Pacific subtropical anticyclone, which is one of the key circulations in the Meiyu precipitation. The traditional method of analyzing the intensity of the subtropical anticyclone is to use the 5880 gpm height contour at 500 hPa only. However, the variation of 5880 gpm contour may be an intense signal at middle levels, and may not be the indicator of the intensity change of the whole circulation. Meiyu precipitation is closely related to the activities of the west Pacific subtropical anticyclone, but the variance features of the anticyclone have not been well studied. The representation index of the anticyclone's intensity and stability at mid-lower levels is still unsatisfactory, and is one topic of this paper.

In the past, more attention was paid to the Meiyu front because it is closely associated with mesoscale convective activities, a dew-point front located in the periphery of the west Pacific subtropical anticyclone, has not been identified. By using the daily $1^\circ \times 1^\circ$ data of the NCEP/NCAR (the National Center for Environmental Prediction/National Center for Atmospheric Research), the three-dimensional structures of the west Pacific subtropical anticyclone will be shown, and the dew-point front will be analyzed. Gao et al. (2002) discussed this dew-point front and briefly analyzed its structural features. Its existence can properly account for the intensity of the subtropical anticyclone at mid-lower levels. The coupling of the dew-point front with the Meiyu front forms a Meiyu front system (MYFS).

The spatial structure and temporal evolution of the dew-point front, and the coupling of the dew-point front with the Meiyu front will be intensively examined in section 2. The formation of the MYFS will be explored with a traditional frontogenesis function in section 3. A summary is given in section 4.

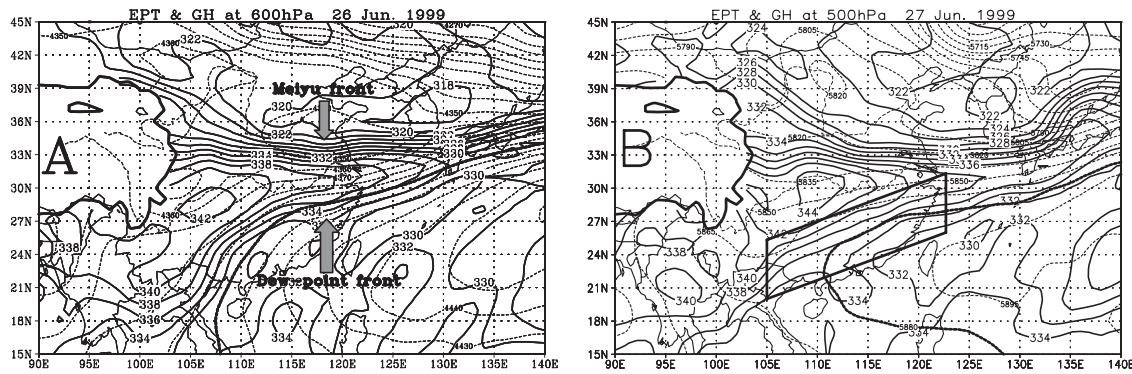


Fig. 1. Distribution of equivalent potential temperature θ_e and geopotential height Φ (A; at 600 hPa at 0000 UTC 26 June 1999, B; at 500 hPa at 0000 UTC 27 June 1999). Solid line: θ_e (units in K), dashed line: Φ (units in gpm) of 4400 gpm in A and 5880 gpm in B, the blank areas indicate areas higher than 4000 m above sea level, and the Meiyu front and the dew-point front are marked by arrows. The region surrounding by a parallelogram in B will be used in Fig. 6.

2. Structural features of the dew-point front and the MYFS

In early summer, when the subtropical anticyclone moves westward and intensifies over continental China, the lower-troposphere temperature increases and the moisture decreases in the periphery of the subtropical anticyclone because of the adiabatic subsidence. As the moist southwest monsoon flow meets the dry subsidence airflow, a sharp moist transitional zone forms. This transitional zone is referred to as a dew-point front. Similar to the Meiyu front, the dew-point front is associated with moisture contrast rather than a temperature contrast, which is indicated by the large gradient zone of equivalent potential temperature θ_e . Figure 1 shows that two clusters of large gradient zones of θ_e isolines are located separately to the north and south side of 30°N. The northern component is the Meiyu front, and the southern one is the dew-point front.

2.1 Spatial structure and temporal evolution of the dew-point front

The dew-point front, a narrow moist transitional zone, was mainly in the mid-lower troposphere. In our study, the definition of the dew-point front is taken into account both the gradient of θ_e and its strength. In detail, at day-by-day maps, besides a large horizontal gradient of θ_e at isobaric surfaces, the 340 K isoline of θ_e at 600 hPa should stretch eastward and cross 110°E. Figure 2 shows that a large meri-

dional gradient of specific humidity and equivalent potential temperature is located around 23–26°N on 20 July, 24–27°N on 24 July, and 25–28°N on 26 July 1998, indicating the dew-point front with a gradual northward propagation within 23–28°N. The humidity ridge and trough lies to the north and south of the dew-point front forming a sharp moisture gradient. The dew-point front is located in the northwest periphery of the west Pacific subtropical anticyclone. The distribution of θ_e in Fig. 2 shows that the dew-point front can be identified more clearly in the mid-lower troposphere (500–700 hPa). The dew-point front covers the large area of East Asia (20–28°N, 105–135°E) and orients southwest-northeast or east-west. The propagation of the dew-point front is associated with the activities of the west Pacific subtropical anticyclone.

Before the mature period of the Meiyu, the dew-point front is rather weak. With the enhancements of both the southwest monsoon flow and the adiabatic subsidence flow in the periphery of the west Pacific subtropical anticyclone, the moisture contrast between the moist southwest monsoon and the dry air near the periphery of the subtropical anticyclone becomes distinct (Figs. 1 and 2). As a result, the dew-point front intensifies during the mature period of the Meiyu. The dew-point front conjugates with the Meiyu front and forms a Meiyu front system (MYFS). The dew-point front starts to decay (not shown) in the late pe-

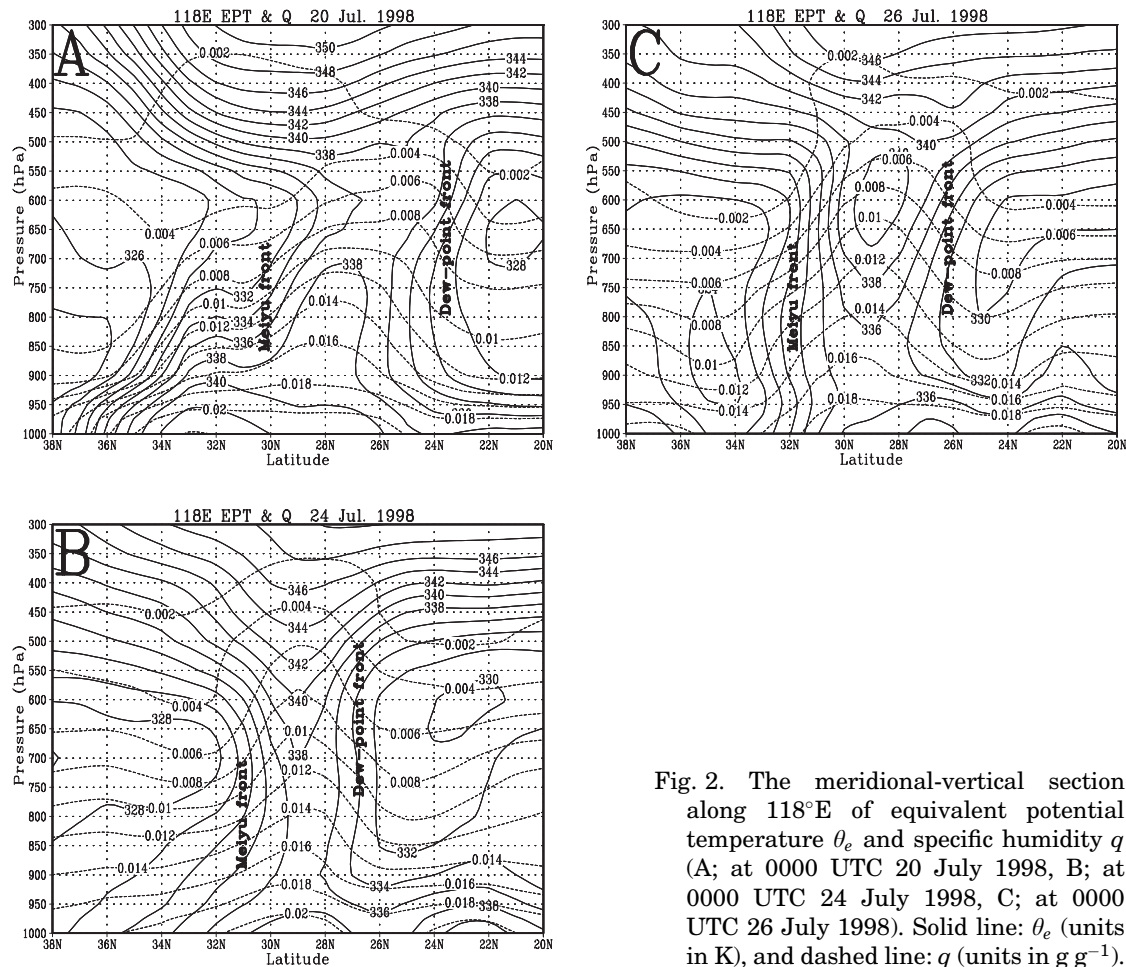


Fig. 2. The meridional-vertical section along 118°E of equivalent potential temperature θ_e and specific humidity q (A; at 0000 UTC 20 July 1998, B; at 0000 UTC 24 July 1998, C; at 0000 UTC 26 July 1998). Solid line: θ_e (units in K), and dashed line: q (units in g g^{-1}).

riod of the mature Meiyu, and vanishes when the Meiyu decays. The above temporal evolution is obtained by analyzing the dew-point front in 1998 and 1999, to draw a general conclusion about the temporal evolution of the dew-point front, more cases need to be analyzed.

2.2 Structures of the MYFS

A passageway is located between the two fronts in the MYFS and orients southwest-northeast. The MYFS starts from the east of the Tibet Plateau and extends along the MRYS in China to Southwest Japan. A high θ_e associated with the MYFS occurs in the mid-lower troposphere. As the MYFS stretches to the east, the dew-point front and the Meiyu front become closer to each other. The MYFS over the ocean is weaker than over the continent. The moisture transport associated with the

MYFS can be examined by the moisture flux ($\mathbf{v}q$) averaged from 22 June to 2 July 1999 at 500, 600, and 700 hPa (Fig. 3). The moisture transport in this period is characterized by southwesterly moisture flux in the passageway of the MYFS at 600–700 hPa and westerly moisture flux at 500 hPa.

From 22 June to 2 July 1999 (the mature period of the Meiyu), large precipitations occurred in the passageway of the MYFS (Fig. 4), which is associated with the large moisture flux ($\frac{1}{g}|\mathbf{v}q|$) (Fig. 5A) and convergence of the moisture flux ($\frac{1}{g}\nabla \cdot (\mathbf{v}q)$) (Fig. 5B), this analysis is consistent with the results of Ninomiya (1999). The water vapor transport and its convergence associated with the low level southwesterly, are parallel to the dew-point front and prevail along the passageway. This causes a strong warm moisture advection toward the Meiyu

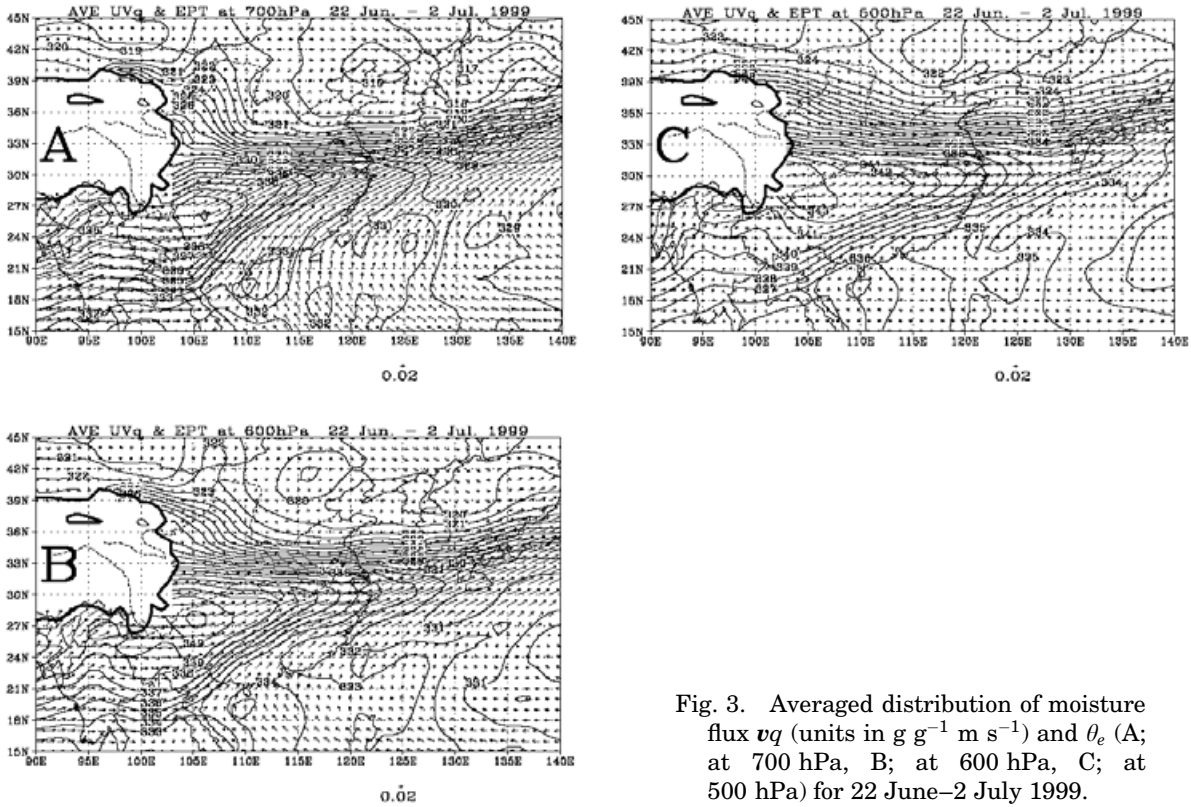


Fig. 3. Averaged distribution of moisture flux vq (units in $g\ g^{-1}\ m\ s^{-1}$) and θ_e (A; at 700 hPa, B; at 600 hPa, C; at 500 hPa) for 22 June–2 July 1999.

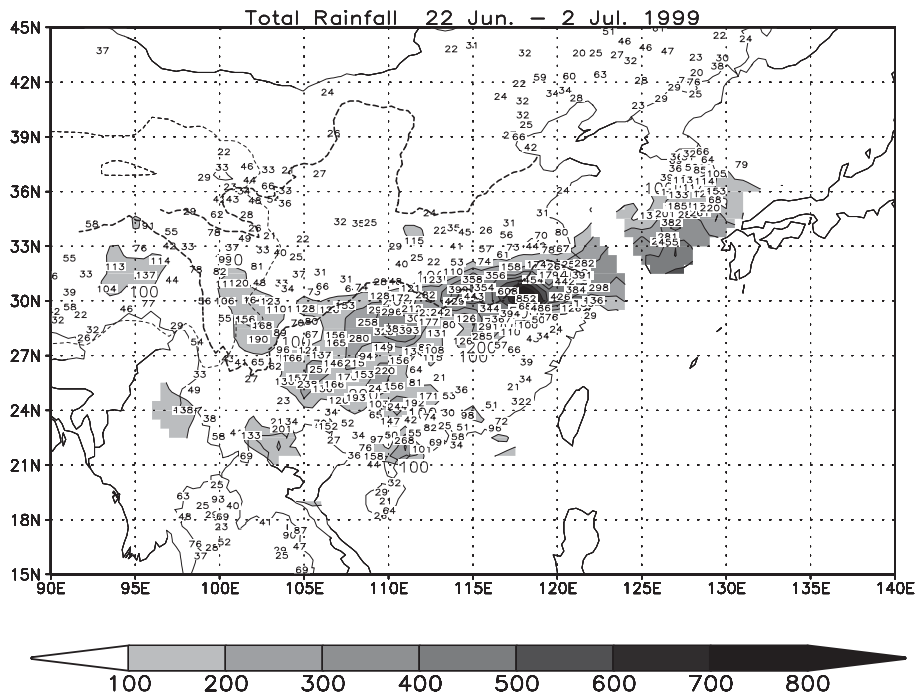


Fig. 4. The total rainfall over the MRYSR observed at 0000 UTC for 22 June–2 July 1999 (units in mm). The shaded regions have the rainfall more than 100.

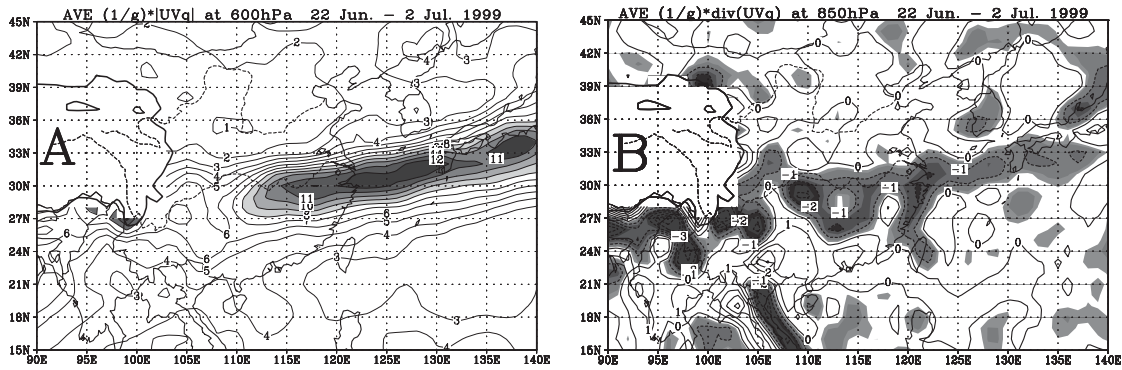


Fig. 5. Averaged distribution of moisture flux $\frac{1}{g}|vq|$ at 600 hPa (A; units in $g s^{-1} cm^{-1} hPa^{-1}$) and moisture flux divergence $\frac{1}{g}\nabla \cdot (vq)$ at 850 hPa (B; units in $10^{-7} g s^{-1} m^{-1} cm^{-1} hPa^{-1}$) for 22 June–2 July 1999. The shaded regions have moisture fluxes more than 8 and moisture flux divergence less than 0.3, respectively.

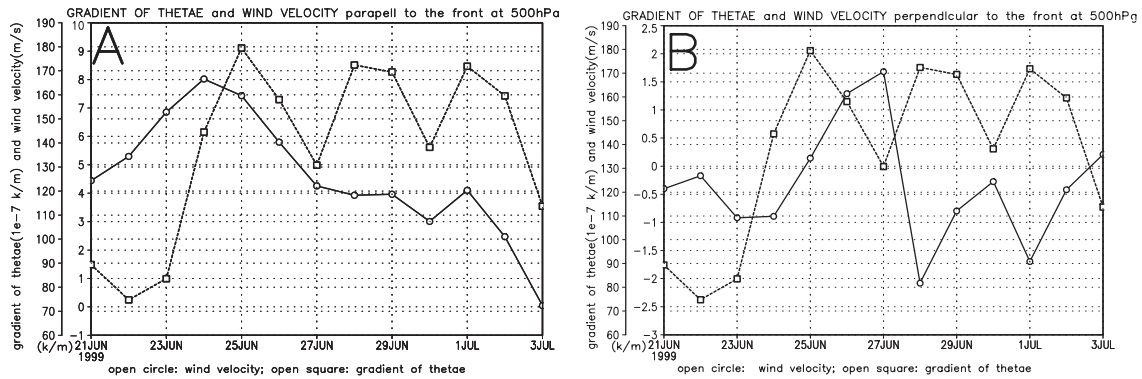


Fig. 6. Temporal variation curves of the horizontal wind parallel to the dew-point front (A; units in $m s^{-1}$), the horizontal wind perpendicular to the dew-point front (B; units in $m s^{-1}$) and the gradient of the equivalent potential temperature (A and B; units in K) at 600 hPa from 20 June to 3 July 1999. The wind velocity and the gradient of θ_e are area averaged in the region of the parallelogram in Fig. 1B.

front and generates thermal instability, which sets the favorite condition for intensification of the Meiyu front. The precipitation is strongly controlled by the circulation associated with the MYFS during the Meiyu period since the moisture over the Bay of Bengal and the South China Sea is transported mainly by the southwest monsoon through the passageway of the MYFS. This concentrated moisture transport leads to a great amount of moisture convergence along the MRYS to Southwest Japan. The moisture convergence maintains a high θ_e in the mid-troposphere in the passageway of the MYFS and is a key factor in the formation and maintenance of the Meiyu front and the dew-point front.

Figure 6 shows temporal evolution of the horizontal wind parallel to the dew-point front (open circle in Fig. 6A), the horizontal wind perpendicular to the dew-point front (open circle in Fig. 6B), and gradient of the equivalent potential temperature (the open square in Figs. 6A and B) averaged within a parallelogram region of the dew-point front (see Fig. 1B). The southwesterly (wind parallel to the dew-point front) is much stronger than southeasterly or northwesterly (wind perpendicular to the dew-point front). Thus, the southwesterly prevails on the dew-point front during the heavy rainfall period. The horizontal wind parallel to the dew-point front is almost in phase with the gradient of the equivalent potential tempera-

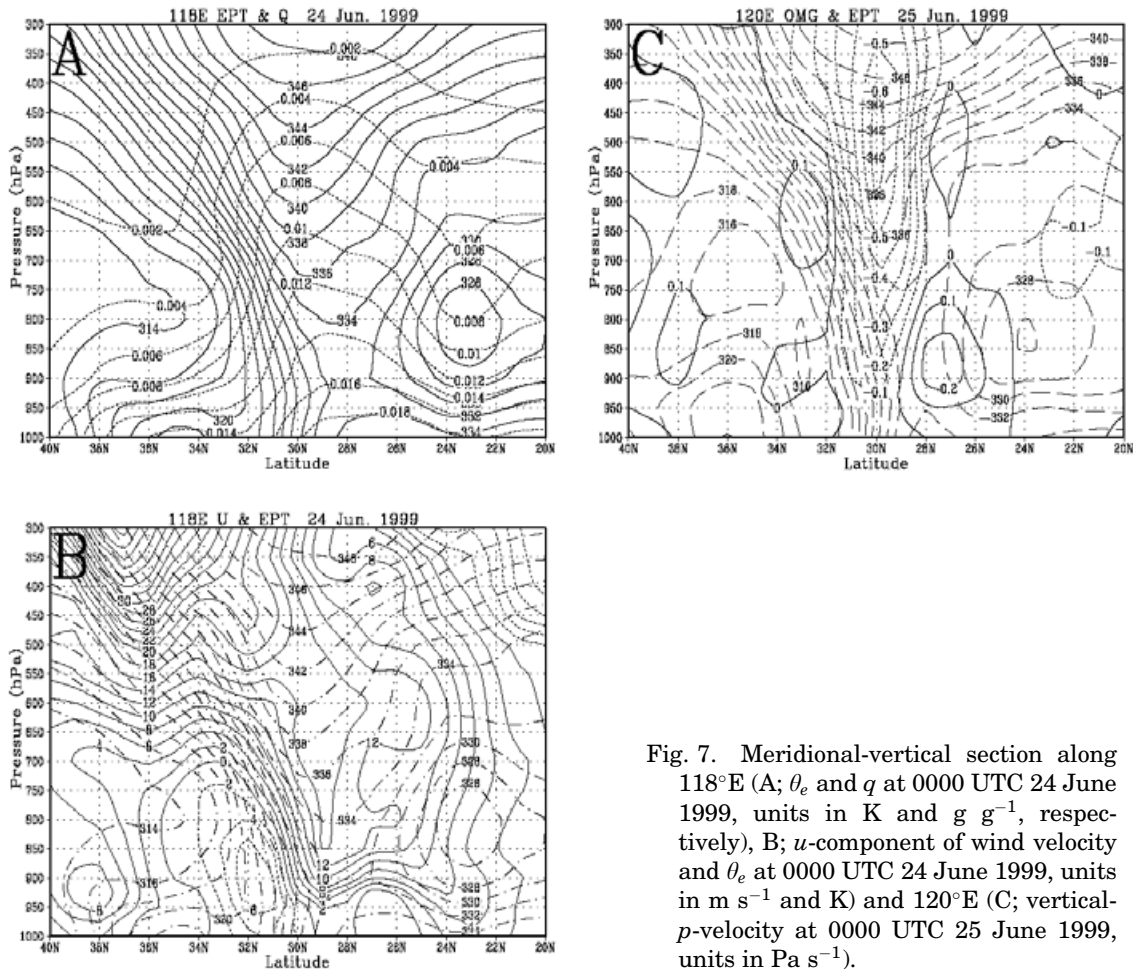


Fig. 7. Meridional-vertical section along 118°E (A; θ_e and q at 0000 UTC 24 June 1999, units in K and $g\ g^{-1}$, respectively), B; u -component of wind velocity and θ_e at 0000 UTC 24 June 1999, units in $m\ s^{-1}$ and K) and 120°E (C; vertical- p -velocity at 0000 UTC 25 June 1999, units in $Pa\ s^{-1}$).

ture (Fig. 6A) whereas the horizontal wind perpendicular to the dew-point front is almost out of phase with the gradient of the equivalent potential temperature (Fig. 6B) from 22 June to 2 July 1999. This implies that the dew-point front accompanies the southwesterly transport of the warm and moist air and prevents the moist flow from penetration.

Figure 7A represents the meridional-vertical section of the MYFS along 118°E at 0000 UTC 24 June 1999. It shows two concentrated θ_e isoline belts. The one in the north (between 29°N and 33°N) corresponds to the Meiyu front, and the other in the south (around 26°N) corresponds to the dew-point front near the periphery of the west Pacific subtropical anticyclone. In the MYFS, a passageway with a remarkably high-valued region of specific humidity q extends from the surface to 300 hPa.

The zonal wind velocity field (Fig. 7B) clearly shows that very strong westerly winds prevail in the upper troposphere (above 300 hPa level) over and to the north of the Meiyu front, and easterly winds appear below 750 hPa level against the north side of the Meiyu front. There is a very strong vertical wind shear between the easterly and the westerly winds near 750 hPa. Over the dew-point front, the easterly winds prevail at 200 hPa, and the southwesterly winds appear below 850 hPa level. This indicates that the horizontal wind associated with the MYFS is vertically asymmetric.

A strong ascending motion (between 32°N and 28°N) is concentrated within the intense rainfall zone (see Figs. 4 and 7C). The upward motion associated with the MYFS is surrounded by the subsidence. Such a descending motion prompts the formation of the dew-point

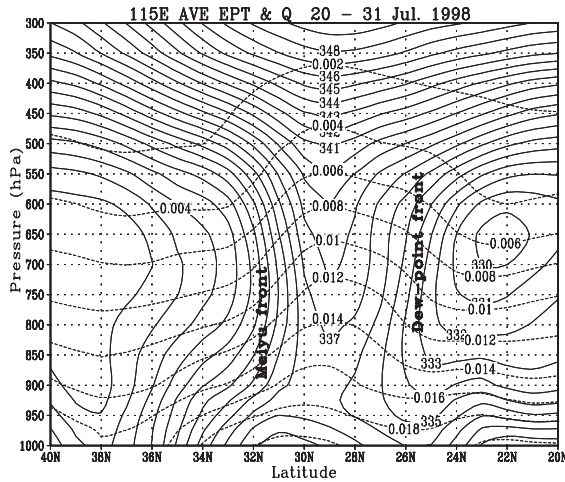


Fig. 8. Averaged meridional-vertical section along 115°E of θ_e (solid line, units in K) and q (dashed line, units in g g^{-1}) for 20–31 July 1998.

front. The maximum ascent speed is as large as 0.7 Pa s^{-1} , which is favorable to the vertical transportation of moisture and forms a humidity ridge in the MYFS. The ascending motion and its adjacent subsidence form the secondary circulation of the MYFS. The strong vertical upward motion in this passageway transports moisture from lower levels to mid-upper levels, this process is responsible for the formation of a relative humidity ridge in the passageway of the MYFS, increasing θ_e and maintaining the MYFS's passageway.

Besides performing day-to-day analyses of the dew-point front and the MYFS, we also analyze the time-mean structure of the MYFS during the last twelve days in July 1998 (from 20 to 31 July). The mean meridional-vertical section along 115°E of the MYFS is shown in Fig. 8. Two areas with large θ_e gradient are evident indicating that the dew-point front could last for more than 10 days and has the time scale similar to the Meiyu front in 1998.

Figures 2, 7 and 8 also show that in the lower troposphere, positive $\partial\theta_e/\partial p > 0$ is associated with the MYFS, which is favorable to the convective development. However, a much thicker layer with a nearly moist natural stratification appears in the mid-lower level of the troposphere within the passageway of the MYFS. To the south of the dew-point front, a region with

low θ_e occurs in the mid-lower troposphere (600–900 hPa in Fig. 2A, 550–800 hPa in Fig. 2B, and 600–800 hPa in Fig. 2C). The low θ_e is caused by the low relative humidity in this region. Stratification in this region is characterized by the high θ_e in the very low levels and inhibited by the low θ_e in the mid-lower levels. This stratification is similar to that occurred in July 1991 and was analyzed by Ninomiya (2000). The low θ_e region corresponds mainly to the dry and warm flow near the ridge axis of the subtropical anticyclone and shifts southwestward when the subtropical anticyclone stretches to the west. Between this low θ_e region and the monsoon flows, a large gradient of θ_e also exists in the lower troposphere from 24°N to 27°N (see Fig. 7A). This gradient zone of θ_e appears each year in the lower troposphere during the Meiyu period because a large moisture contrast always forms between the warm and moist southwest monsoon and the dry air in the subtropical anticyclone over this region (Zhou 2002). When the west Pacific subtropical anticyclone becomes strong, it elongates westward and its ridge line moves northward, this makes the gradient of θ_e in the lower level connect with the dew-point front in the middle troposphere and integrates into a whole front from the lower to the mid troposphere. This explains why the dew-point front (Figs. 2 and 8) was stronger in 1998 than in 1999 (Fig. 7). The subtropical anticyclone was much stronger and its ridge line was located far more north in 1998 than in 1999 (Zhou 2002). This supports the argument made in the introduction that the occurrence of the dew-point front in the mid-lower troposphere is associated with the intensification of the west Pacific subtropical anticyclone in the mid-lower level. Generally, between 700 hPa and 500 hPa, negative $\frac{\partial\theta_e}{\partial y}$ is associated with the Meiyu front, whereas positive $\frac{\partial\theta_e}{\partial y}$ is associated with the dew-point front because of the high θ_e in the MYFS's passageway. Once the dew-point front is enhanced in the mid-lower troposphere, a 'double front' structure (consisting of the Meiyu front and the dew-point front) should occur (see Figs. 2 and 8). Figures 2B, C and Fig. 7B show that in the lower troposphere, there exist a weak local maximum of θ_e and q between 21°N and 24°N (Figs. 2B and C) and a local maximum of u between 22°N and 25°N (Fig. 7B), which may be

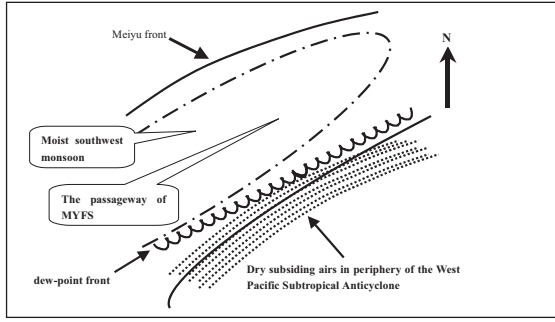


Fig. 9. A conceptual model of the Meiyu front system.

associated with the lower level jet (LLJ) during the Meiyu period. This analysis will be reported in a separate paper.

Based upon the above analyses, a conceptual model of the MYFS is constructed in Fig. 9. In this model, the dew-point front appears between the southwest monsoon and the dry subsiding air near the periphery of the west Pacific subtropical anticyclone. The Meiyu front appears to the north of the dew-point front. The analyses show that although the dew-point front does not play an essential role in the formation and development of the Meiyu front, it favors the transport of the warm and moist southwest monsoon flow along the passageway of the MYFS. Since the upward motion transports the moist air to the upper troposphere, a narrow humidity ridge forms. As the moist air moves to the upper levels in the passageway of the MYFS, the instability develops along the MRYS, which causes strong convection and heavy rain. However, the dew-point front has interannual variability. The dew-point front was weak in 2000 and did not appear in 2001 (Gao et al. 2002) due to the dry summers, while the Meiyu fronts appeared but were weaker than those in 1998 and 1999. This indicates that the development of the dew-point front is in phase with the development of the Meiyu front and the west Pacific subtropical anticyclone strengthen, and the dew-point front is a part of the MYFS. Its genesis and development are determined by the moisture transports along the passageway. The warm moisture advection toward the Meiyu front favors the development of the dew-point front and generates thermal instability, and the instability en-

hances the Meiyu front. The genesis and development of the dew-point front are strong indicators of the development of the Meiyu front and the west Pacific subtropical anticyclone. The formation of the dew-point front in 1998 and 1999 is further examined to show a strong Meiyu always accompanies the dew-point front.

3. Diagnostic analyses of the formation of the MYFS

By using a frontogenesis function, Ninomiya (1984, 2000) and Sun and Du (1996) analyzed the frontogenesis of the Meiyu front and found that the large-scale confluence and deformation of the horizontal wind in the front contributes to the formation of the Meiyu front. The traditional frontogenesis function used to analyze the frontogenesis of the Meiyu front is as follows (Ninomiya 1984).

$$FG \equiv \frac{d|\nabla\theta_e|}{dt} = FG1 + FG2 + FG3 + FG4 \quad (3.1)$$

where $FG1$, $FG2$, $FG3$, and $FG4$ are defined as:

$$FG1 = \frac{1}{|\nabla\theta_e|} \left[(\nabla\theta_e \cdot \nabla) \frac{d\theta_e}{dt} \right] \quad (3.2)$$

$$FG2 = -\frac{1}{2} \frac{1}{|\nabla\theta_e|} (\nabla\theta_e)^2 \left(\frac{\partial u}{\partial x} + \frac{\partial v}{\partial y} \right) \quad (3.3)$$

$$FG3 = -\frac{1}{2} \frac{1}{|\nabla\theta_e|} \left[\left(\frac{\partial\theta_e}{\partial x} \right)^2 - \left(\frac{\partial\theta_e}{\partial y} \right)^2 \right] \left(\frac{\partial u}{\partial x} - \frac{\partial v}{\partial y} \right) + 2 \frac{\partial\theta_e}{\partial x} \frac{\partial\theta_e}{\partial y} \left(\frac{\partial v}{\partial x} + \frac{\partial u}{\partial y} \right) \quad (3.4)$$

$$FG4 = -\frac{1}{|\nabla\theta_e|} \frac{\partial\theta_e}{\partial p} \left(\frac{\partial\theta_e}{\partial x} \frac{\partial\omega}{\partial x} + \frac{\partial\theta_e}{\partial y} \frac{\partial\omega}{\partial y} \right) \quad (3.5)$$

here, θ_e is equivalent potential temperature, u is the zonal wind component, v is the meridional wind component and ω is the vertical- p -velocity component, while $FG1$ is the diabatic heating term, $FG2$ is the convergence term, $FG3$ is the deformation term, and $FG4$ is the slantwise term.

Figures 10A and B show the synthetic distribution of $FG2$ and $FG3$ at 600 hPa at 0000 UTC 26 June and its averaged distribution from 22 June to 2 July 1999, respectively. In these two figures, two positive value zones along the north and south side of the Yangtze river Basin, extending from the eastern side

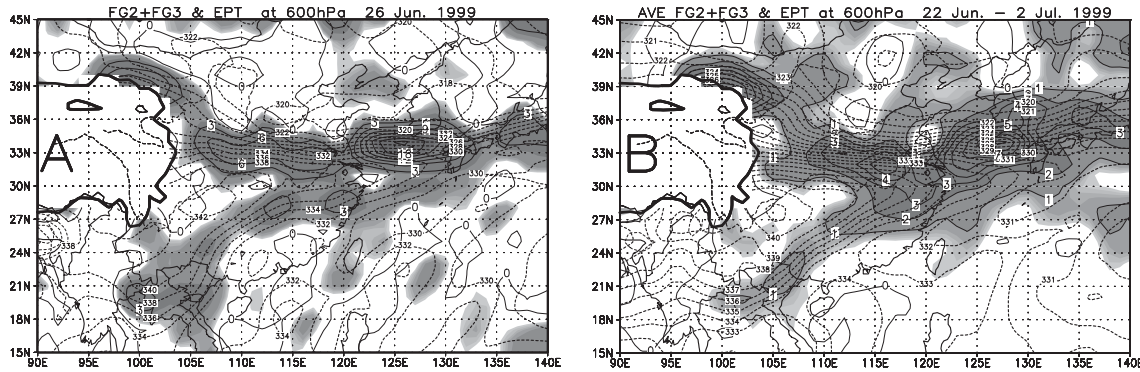


Fig. 10. The distribution of $FG2 + FG3$ (units in $10^{-10} \text{ K m}^{-1} \text{ s}^{-1}$) at 0000 UTC 26 June 1999 (A) and its averaged distribution for 22 June–2 July 1999 (B) at 600 hPa. The shaded region has $FG2 + FG3 \geq 0.01$.

and southern side of the Tibetan Plateau to the East China Sea and the southwest of Japan, which correspond to frontogenesis of the Meiyu front and the dew-point front, respectively. Though the frontogenesis zone corresponding to the dew-point front is weaker than frontogenesis of the Meiyu front (whose values of $FG2 + FG3$ is less than that of the Meiyu front), it still can reflect the frontogenesis of the dew-point front. Similar to the MYFS, two frontogenesis zones also combine to one when they stretch from west to east. Though the $FG1$ and $FG4$ are negative near the two fronts (figures not shown), the large-scale convergence and deformation of the horizontal wind in the frontal zone work together to sustain the strong gradient of θ_e against the decrease of θ_e caused by the diabatic heating and the convective transport, it manifests that the deformation term $FG3$ and the convergence term $FG2$ are predominant among the four terms, and this result agrees with studies of Ninomiya (1984, 2000) and Sun and Du (1996).

4. Summary

Analyses of the NCEP/NCAR daily $1^\circ \times 1^\circ$ data demonstrates the existence of the dew-point front. The variation of the dew-point front position is related to the activities of the west Pacific subtropical anticyclone. The coupling of the dew-point front with the Meiyu front forms the MYFS that leads to a strong Meiyu. A conceptual model of the MYFS is provided (Fig. 9)

based on the analyses. The Meiyu front is the north branch of the MYFS, located at $30\text{--}35^\circ\text{N}$ and stretching from the MRYSR in China to Southwest Japan. And the dew-point front is the south branch of the MYFS. Generally, the dew-point front orients southwest-northeast in ($20\text{--}28^\circ\text{N}$, $105\text{--}135^\circ\text{E}$, $500\text{--}700$ hPa). Analysis of the structures of the MYFS shows that westerly and easterly winds prevail in the lower and upper troposphere along the dew-point front whereas easterly and westerly winds prevail in the lower and upper troposphere along the Meiyu front. The upward motion in the passageway of the MYFS is surrounded by the downward motion, forming the secondary circulation of the MYFS. By using a traditional frontogenesis function, the large-scale confluence and deformation of the horizontal wind are found to play important roles in the formation and development of the Meiyu front and the dew-point front.

Although the structural and frontogenesis analyses of the dew-point front are analyzed, more works, for example, the development of severe convective systems and associated torrential rains in the MYFS, what causes strengthening of subtropical anticyclone in the seasonal march or interannually, need to be further studied. Nevertheless, the study establishes the dynamic framework for further research on the dew-point front, and provides the background for the improvement of forecasting the torrential rain during the Meiyu period.

Acknowledgement

The authors wish to thank the three referees for their constructive suggestions that substantially improved this paper. In particular, we thank the referee who suggested a conceptual model of the MYFS, which is presented as Fig. 9 in this paper. This work was supported by the projects of National Natural Science Foundation of China (Nos. 40405007 and 40205010) and Chinese Academy of Sciences (No. KZCX3-SW-213). Shen was supported in part by the "Outstanding Overseas Chinese Scholars" project of the Chinese Academy of Sciences under grant No. 2002-1-2, two OGP grants from the United States NOAA, and a Canadian MITACS research grant.

References

- Akiyama, T., 1973: The large-scale aspects of the characteristic features of the Baiu front. *Pap. Meteor. Geophys.*, **24**, 157–188.
- , 1984a: A medium-scale cloud cluster in a Baiu front, part I: Evolution process and fine structure. *J. Meteor. Soc. Japan*, **62**, 485–504.
- , 1984b: A medium-scale cloud cluster in a Baiu front, part II: Thermal and kinematic fields and heat budget. *J. Meteor. Soc. Japan*, **62**, 505–521.
- , 1987: Conceptual models of Baiu front and Baiu front disturbances in multi-scale characteristics. *Mesoscale Analysis & Forecasting. Proceedings of an International Symposium*. Vancouver, Canada, 17–19 August 1987, 195–200.
- , 1989: Large, synoptic and meso scale variations of the Baiu front during July 1982, part I: Cloud features. *J. Meteor. Soc. Japan*, **67**, 57–80.
- , 1990: Large, synoptic and meso scale variations of the Baiu front during July 1982, part II: Frontal structure and disturbances. *J. Meteor. Soc. Japan*, **68**, 557–574.
- Chen, Z., 1992: The dynamical diagnosis of heavy rain exploded by the imbalance motion in atmosphere (in Chinese). *Chi. Sci. Bull.*, **37**, 1342–1343.
- Gao, S., S. Tao, and Y. Ding, 1990: The generalized E-P flux of wave-meanflow interactions. *Sci. Chin. (Series B)*, **33**, 704–715.
- Gao, S., Y. Zhou, and T. Lei, 2002: Structural features of the Meiyu front system. *ACTA METEOROLOGICA SINICA*, **16**, 195–204.
- Hu, B., 1997: The band of CISK coupled with low level "moisture fronts" and the genesis of warm shear line-type Meiyu fronts (in Chinese). *Sci. Atmos. Sin.*, **21**, 679–686.
- Iwasaki, H., and K. Takeda, 1993: Structure and behavior of mesoscale cloud clusters traveling over the Baiu-front zone. *J. Meteor. Soc. Japan*, **71**, 733–747.
- Kitabatake, N., 2000: Structure of the Baiu (Meiyu) front over China continent: A lower dryline-like front coupled with an upper front (in Japanese). *Tenki*, **47**, 555–567.
- Lin, C., 1979: Meiyu and its forecast in mid-lower reaches of Yangtze River (in Chinese). *Meteorological Monthly*, **53**, 2–8.
- Lin, Y., and Q. Wu, 2000: Reviews on the study of the subtropical anticyclone and new insights on some fundamental problems (in Chinese). *ACTA METEOROLOGICA SINICA*, 2002, **58**, 500–512.
- Matsumoto, S., S. Yoshizumi, and M. Takeuchi, 1970: On the structure of the Baiu front and associated intermediate-scale disturbances in the lower atmosphere. *J. Meteor. Soc. Japan*, **48**, 479–491.
- , K. Ninomiya, and S. Yoshizumi, 1971: Characteristic features of Baiu front associated with heavy rainfall. *J. Meteor. Soc. Japan*, **49**, 267–281.
- Ninomiya, K., 1984: Characteristics of Baiu front as a predominant subtropical front in the summer northern hemisphere. *J. Meteor. Soc. Japan*, **62**, 880–893.
- , 1999: Moisture balance over China and the South China Sea during the summer monsoon in 1991 in relation to the intense rainfalls over China. *J. Meteor. Soc. Japan*, **77**, 737–751.
- , 2000: Large- and meso-scale characteristics of Meiyu/Baiu front associated with intense rainfalls in 1–10 July 1991. *J. Meteor. Soc. Japan*, **78**, 141–157.
- , and T. Akiyama, 1992: Multi-scale features of Baiu. The summer monsoon over Japan and the East Asia. *J. Meteor. Soc. Japan*, **70**, 467–495.
- , and K. Kurihara, 1987: Forecast experiment of long-lived convective system in Baiu frontal zone. *J. Meteor. Soc. Japan*, **65**, 885–899.
- , and K. Yamazaki, 1979: Heavy rainfalls associated with frontal depress in Asia subtropical humid region (II): Mesoscale features of precipitation. *J. Meteor. Soc. Japan*, **57**, 399–413.
- , T. Akiyama, and M. Ikawa, 1988: Evolution and fine structure of a long-lived meso- α -scale convective system in Baiu frontal zone, Part I: Evolution and meso- β -scale characteristics. *J. Meteor. Soc. Japan*, **66**, 331–350.
- , T. Akiyama, and M. Ikawa, 1988: Evolution and fine structure of a long-lived meso- α -scale

- convective system in Baiu frontal zone, Part II: Meso- γ -scale characteristics of precipitation. *J. Meteor. Soc. Japan*, **66**, 351–371.
- Sun, S., and C. Du, 1996: The maintenance of the Meiyu front and development of associated disturbances (in Chinese). *J. Appl. Meteor. Sci.*, **7**, 153–159.
- Tao, S., 1958: Meiyu in China, in *Proceedings of Meteorology* (in Chinese), Chinese Meteorological Press, 36 pp.
- Zhang, B., and Z. Zhang, 1990: *A study on heavy rain of Meiyu front in mid-lower reaches of Yangtze River* (in Chinese). Chinese Meteorological Press, 272 pp.
- Zhou, Y., 2002: Study on the spatical structural features and its forming mechanism of the Meiyu front system and moist potential vorticity anomaly (in Chinese), Ph.D. thesis, Institute of Atmospheric Physics, Chinese Academy of Sciences, 189 pp.